chemengineering

MDPI

Article

Application of Response Surface Methodology for H_2S Removal from Biogas by a Pilot Anoxic Biotrickling Filter

Fernando Almenglo *, Martín Ramírez * and Domingo Cantero

Department of Chemical Engineering and Food Technologies, Wine and Agrifood Research Institute (IVAGRO), Faculty of Sciences, University of Cádiz, 11510 Puerto Real (Cádiz), Spain

* Correspondence: fernando.almenglo@uca.es (F.A.); martin.ramirez@uca.es (M.R.); Tel.: +34-956016286 (M.R.)

Received: 13 May 2019; Accepted: 11 July 2019; Published: 13 July 2019

Abstract: In this study, a pilot biotrickling filter (BTF) was installed in a wastewater treatment plant to treat real biogas. The biogas flow rate was between 1 and 5 $m^3 \cdot h^{-1}$ with an H_2S inlet load (*IL*) between 35.1 and 172.4 $gS \cdot m^{-3} \cdot h^{-1}$. The effects of the biogas flow rate, trickling liquid velocity (*TLV*) and nitrate concentration on the outlet H_2S concentration and elimination capacity (*EC*) were studied using a full factorial design (3^3). Moreover, the results were adjusted using Ottengraf's model. The most influential factors in the empirical model were the *TLV* and H_2S *IL*, whereas the nitrate concentration had less influence. The statistical results showed high predictability and good correlation between models and the experimental results. The R-squared was 95.77% and 99.63% for the '*C model*' and the '*EC model*', respectively. The models allowed the maximum H_2S *IL* (between 66.72 and 119.75 $gS \cdot m^{-3} \cdot h^{-1}$) to be determined for biogas use in a combustion engine (inlet H_2S concentration between 72 and 359 ppm_V). The '*C model*' was more sensitive to *TLV* (–0.1579 $(gS \cdot m^{-3})/(m \cdot h^{-1})$) in the same way the '*EC model*' was also more sensitive to *TLV* (4.3303 $(gS \cdot m^{-3})/(m \cdot h^{-1})$). The results were successfully fitted to Ottengraf's model with a first-order kinetic limitation (R-squared above 0.92).

Keywords: hydrogen sulfide; anoxic biotrickling filter; biogas; Ottengraf's model; open polyurethane foam; response surface methodology

1. Introduction

Biogas, due to methane high combustion enthalpy, can be considered as an important renewable energy source. Nowadays, international laws such as the Directive of the European Parliament 2009/28/EC (April 23, 2009) recognize biogas as a source of vital energy that can reduce the European Union's energy dependence. The aim of this directive is to increase consumption of renewable energy by 2020 by at least 20%. The longer-term goal is to achieve net-zero greenhouse emissions by 2050 and it will be necessary to increase investment in clean and energy-efficient technologies by 2.8% of Gross Domestic Product (GDP) (or around € 520–575 billion annually) [1]. Hydrogen sulfide (H_2S) is one of the biggest pollutants in biogas. Therefore, it is necessary to reduce the generation of H_2S in the digester and/or reduce its concentration for most uses of biogas. Apart from its harmful effects on health, the presence of H_2S in biogas is not desirable because it is a corrosive gas. Desulfurization of biogas can be carried out by physical-chemical or biological processes. Physical-chemical processes have been commonly used but biological ones have proven to be a good competitor from economic and environmental points of view [2].

In biological processes the most widely used and studied microorganisms belong to the group of bacterial chemotrophic species, which use reduced sulfur compounds as an energy source and use oxygen (aerobic) or nitrate/nitrite (anoxic) as electron acceptors [3,4]. The biodesulfurization of biogas

involves the use of technologies that facilitate appropriate contact between the gas and the liquid. There are several advantages in the use of anoxic biotrickling filters (BTFs) over aerobic ones, and these include reducing the risk of explosion, no dilution of biogas, and a lower limitation in the transfer of matter for nitrate when compared to the necessary oxygen absorption [5,6]. In contrast, the cost and availability of large amounts of nitrate can be limiting for the application of anoxic systems. Although ammonia-rich wastewater could be nitrified and used, Zeng et al. [3] used a biogas digestion slurry after nitrification to feed a BTF to achieve stable operation.

The H_2S inlet load (*IL*) in BTFs is an important parameter in the design of this type of equipment. The *IL* and the elimination capacity (*EC*) describe the performance of the BTFs with respect to the removal efficiency (*RE*) of the contaminant and allow the design of the system, depending on the biogas flow rate that needs to be treated and the inlet H_2S concentration. Values for a critical *EC* of between 100 and 130 $gS{\cdot}m^{-3}{\cdot}h^{-1}$ and a maximum *EC* between 140 and 280 $gS{\cdot}m^{-3}{\cdot}h^{-1}$ have been reported for both aerobic and anoxic biotrickling filters [5,7].

A model can be applied to relate input variables (pollutant inlet concentration, gas flow, electron acceptor concentration, etc.) and design variables (specific surface area of the support, equipment dimensioning, etc.) with the outputs (concentration of the pollutant at the outlet, production of biological reaction products, consumption of reagents, etc.). Empirical models (black box models) are characterized by a high predictive power, but their parameters lack physical significance [8]. They are based on statistically significant relationships between the input and output variables. Stationary-state models have been used to describe biofilters since the early 1980s [9–11]. Anoxic BTFs have been described by empirical [12,13] and dynamic [14,15] models. For instance, Soreanu et al. [13] proposed a second-order empirical model using a central composite design (CCD) and the biogas flow rate and the H_2S concentration as input variables, with the H_2S *RE* obtained as a response variable. Almenglo et al. [15] developed a model that considered the most relevant phenomena such as advection, absorption, diffusion and biodegration. Dynamic models provide a better understanding of the process, but their complexity means that they are seldom used for BTFs.

The aim of the work described here was to study the effects of gas (F_G) and liquid (F_L) flow rates and nitrate concentration ($[N\text{-}NO_3^-]$) along the packed bed on the outlet H_2S concentration and the *EC*. Two empirical models were proposed to describe the outlet H_2S concentration and the *EC*. Moreover, the H_2S concentrations were measured along the bed and fitted using Ottengraf's model [9].

2. Materials and Methods

2.1. Experimental Set-up

An anoxic BTF at pilot scale (Figure 1) was installed in the wastewater treatment plant (WWTP) 'Bahía Gaditana' (San Fernando, Spain) and it was fed with biogas from one of their sludge anaerobic digesters. The internal diameter was 0.5 m and the bed height was 0.85 m. The BTF was packed with open-pore polyurethane foam cubes (800 units, 25 $kg{\cdot}m^{-3}$, 600 $m^2{\cdot}m^{-3}$) (Filtren TM25450, Recticel Iberica, Spain). The recirculation medium pH was kept at 7.4 and the temperature at 30 °C.

The nitrate feeding was done in batch mode and automatized by oxide reduction potential (ORP) (setpoint of −365 mV) [16]: when nitrate was exhausted a fixed liquid volume (25 L) was purged, then a nitrate solution (500 $gNaNO_3{\cdot}L^{-1}$) was added to the recirculation medium and finally treated water from the WWTP was added to get a working volume. The nitrate depletion time (NDT) was the time between nitrate feedings, i.e., the time in which microorganisms consumed the nitrate added. NDT was dependent of *IL* and maximum nitrate concentration reached in the nitrate feeding cycle. The volume of the nitrate solution added was modified in concordance to maintain an NDT between 3 and 4 h. This volume ranged in a linear manner between 0.14 and 0.7 L for an H_2S *IL* between 33.3 and 177 $gS{\cdot}m^{-3}{\cdot}h^{-1}$. During the nitrate depletion time the H_2S concentrations in the outlet stream and along the bed height (0.2, 0.4, 0.6 and 0.8 m) were measured every 30 min, and samples of the recirculation medium were taken for nitrate, nitrite and sulfate measurement. Further information about the system

can be found elsewhere [15,16]. A schematic representation of the experimental set-up is provided in Figure 2.

Figure 1. Photograph of the pilot scale anoxic biotrickling filter.

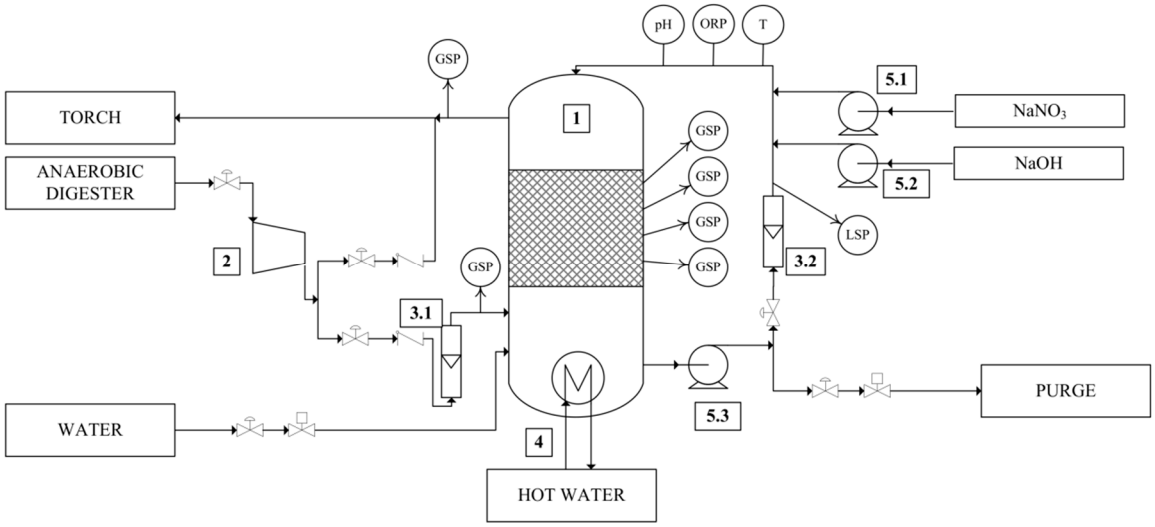

Figure 2. Experimental set-up. GSP—Gas Sampling Port; LSP—Liquid Sampling Port. 1: Biotrickling filter; 2: biogas compressor; 3: rotameters (3.1: biogas and 3.2 liquid); 4: Cryostat Bath; 5: pumps (5.1 $NaNO_3$; 5.2 NaOH; 5.3 recirculation pump).

The H_2S concentration in the biogas stream was measured using a gas chromatograph with a thermal conductivity detector (GC-450, Bruker, Germany) and a specific gas sensor (GAsBadge®Pro, Industrial Scientific, USA) was used for H_2S concentrations below 500 ppm_V. Sulfate, nitrite and

nitrate were measured by a turbidimetric method (4-500-SO_4^{2-} E), a colorimetric method (45000-NO_2^- B) and by an ultraviolet method (4500-NO_3^- B), respectively [17].

2.2. Experimental Design

A response surface model from a full factorial three-level three-factor design (3^3) was developed including two replicates at the central point. 3^3 design allows us to obtain a second-order polynomial using only three levels [18,19]. The three factors were gas flow rate (F_G), liquid flow rate (F_L) and nitrate concentration. The levels of the factor studied, and the values calculated for H_2S *IL* (Equation (1)), trickling liquid velocity (*TLV*) (Equation (2)) and empty bed residence time (*EBRT*) (Equation (3)) are provided in Table 1.

$$IL = \frac{F_G}{V} \cdot [H_2S]_i \quad (1)$$

$$TLV = \frac{F_L}{A}, \quad (2)$$

$$EBRT = \frac{V}{F_G}, \quad (3)$$

$$EC = IL \cdot RE, \quad (4)$$

$$RE = \frac{[H_2S]_i - [H_2S]_o}{[H_2S]_i}, \quad (5)$$

where *IL* is the inlet load ($gS \cdot m^{-3} \cdot h^{-1}$), *V* is the bed volume (m^3), $[H_2S]_i$ is the inlet H_2S concentration ($gS \cdot m^{-3}$), $[H_2S]_o$ is the outlet H_2S concentration ($gS \cdot m^{-3}$), *RE* is the removal efficiency, *EC* is the elimination capacity, *TLV* is the trickling liquid velocity ($m \cdot h^{-1}$), *EBRT* is the empty bed residence time (s) and *A* is the cross-sectional area of the bed (m^2).

Table 1. Levels of the factor tested in the experimental design (3^3).

Factor	Levels of Factors		
	(–1)	**(0)**	**(+1)**
F_G ($m^3 \cdot h^{-1}$)	1	3	5
F_L ($m^3 \cdot h^{-1}$)	1	2	3
$[N\text{-}NO_3^-]$ ($mg \cdot L^{-1}$)	1.4 ± 1.1	35.3 ± 2.4	70.5 ± 10.2
IL [1] ($gS \cdot m^3 \cdot h^{-1}$)	35.1 ± 1.5	109.1 ± 11.7	172.4 ± 3.4
TLV [2] ($m \cdot h^{-1}$)	5.09	10.18	15.27
EBRT [1] (s)	600	200	120

[1] Values calculated for F_G values of 1, 2, and 5 $m^3 \cdot h^{-1}$, respectively, [2] Values calculated for F_L values of 1, 2 and 3 $m^3 \cdot h^{-1}$, respectively.

The experimental results were fitted with two empirical models. The first model, the concentration model ('*C model*'), fitted the outlet H_2S concentration as a response variable. The second model, the elimination capacity model ('*EC model*'), fitted the *EC* as a response variable. In both models the independent variables were *TLV*, the H_2S *IL* and the nitrate concentration (factors from Table 1). Instead of F_G, H_2S *IL* was chosen because the *IL* included the effect of the inlet H_2S concentration (Equation (1)). In addition, *TLV* was used rather than F_L because it allows a comparison with other BTFs. In both cases a second-order polynomial model was used to predict the outlet H_2S concentration and the *EC* values. The data were analyzed using Statgraphics® Centurion XVIII (v.18.1.10).

2.3. Ottengraf's Model

Ottengraf's model [9,20] describes the concentration of pollutants in biofilters for steady-state processes. The analytical solution of the model was obtained in three ideal situations:

1. There is no diffusion limitation and the biofilm is fully active, and hence the conversion rate is controlled by a zero-order reaction rate. The solution is described by Equation (6). K_0 is a pseudo zero-order rate ($g{\cdot}m^{-3}{\cdot}s^{-1}$) and is proportional to the zero-order reaction rate constant (k_0, Equation (7)).
2. There is diffusion limitation and therefore the mass transfer rate to the biofilm is insufficient compared to biological substrate utilization rate. The solution is described by Equation (8).
3. There is no diffusion limitation and the biofilm is fully active, and hence the conversion rate is controlled by a first-order reaction rate. The solution is described by Equation (6). K_1 is a pseudo first-order rate constant (s^{-1}) (Equation (10)) and is proportional to the first-order rate constant (k_1, Equation (10)).

$$\frac{[H_2S]}{[H_2S]_0} = 1 - \frac{K_0{\cdot}H}{[H_2S]_0{\cdot}U_G}, \quad (6)$$

$$\text{With, } K_0 = \delta{\cdot}A_S{\cdot}k_0, \quad (7)$$

$$\frac{[H_2S]}{[H_2S]_0} = \left[1 - \frac{H}{U_G}\sqrt{\frac{A_S{\cdot}K_0{\cdot}D'}{2{\cdot}[H_2S]_0{\cdot}m{\cdot}\delta}}\right]^2, \quad (8)$$

$$\frac{[H_2S]}{[H_2S]_0} = exp\left(-\frac{H{\cdot}K_1}{m{\cdot}U_G}\right), \quad (9)$$

$$\text{With, } K_1 = A_S{\cdot}D'/\delta{\cdot}\phi{\cdot}\tanh\phi, \text{ and } \phi = \delta\sqrt{k_1/D'} \quad (10)$$

where, H is the height of the tower (m), $[H_2S]_0$ is the inlet concentration ($g{\cdot}m^{-3}$), U_G is the superficial gas velocity ($m{\cdot}s^{-1}$), A_S is the specific area ($m^2{\cdot}m^{-3}$), δ is the biofilm thickness (m), m is the distribution coefficient at equilibrium ($m = G_G/C_L$) and D' is the effective diffusion coefficient ($m^2{\cdot}s^{-1}$).

3. Results and Discussion

3.1. Empirical Model

The sulfate and nitrite concentrations were almost constant during the experiments; the sulfate concentration was 8.9 ± 1.6 $gS\text{-}SO_4{\cdot}L^{-1}$ and nitrite concentration was between 0.1 and 10 $mgN\text{-}NO_2^-{\cdot}L^{-1}$. The H_2S *RE* obtained during the experimentation carried out to obtain the empirical model is shown in Figure 3.

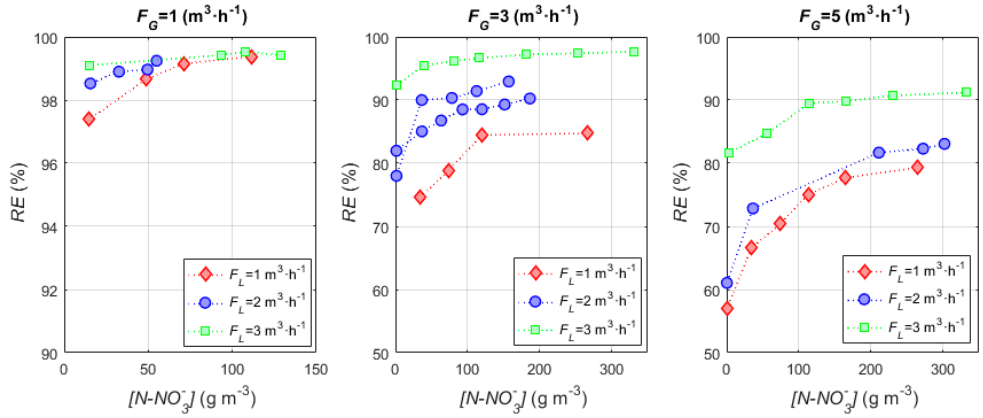

Figure 3. Removal efficiency (*RE*) versus nitrate concentrations at different biogas (F_G) and recirculation (F_L) flow rates.

As expected, a high H_2S *RE* was found at low F_G (lower H_2S *IL*). Therefore, the best results were for an F_G of 1 $m^3{\cdot}h^{-1}$, where the H_2S *IL* was 35.1 ± 1.5 $gS{\cdot}m^{-3}{\cdot}h^{-1}$ and the *RE* between 97.3 and 99.5%.

Under these conditions, the effects of the nitrate concentration and *TLV* were negligible. However, at higher biogas flow rates the decrease in the nitrate concentration led to a lower H_2S *RE*. In anoxic biofiltration nitrate (or nitrite) is the electron acceptor, so its concentration must be a significant factor on the BTF performance, and this is even more important considering that the use of a nitrate feed controlled by ORP [16] leads to a decrease in the nitrate concentration until depletion.

The *RE* versus the *TLV* values for the three F_G (*EBRT* of 600, 200 and 120 s) are listed in Table 2. When the nitrate concentration was not limiting, the *TLV* effect on H_2S *RE* was only notable for an F_G equal to or greater than 3 $m^3 \cdot h^{-1}$ (i.e. for H_2S *IL* of 109.1 ± 11.7 and 172.4 ± 3.4 $gS \cdot m^{-3} \cdot h^{-1}$). Thus, for an F_G of 3 $m^3 \cdot h^{-1}$, the H_2S was between 84.7 and 97.6% and for 5 $m^3 \cdot h^{-1}$ the range was between 79.3 and 92.1%. The improvement observed could be explained by various effects: a higher wetted area [21], an increase in the hold-up liquid (6.4, 8.5 and 10.6 L for 5.1, 10.2 and 15.3 $m \cdot h^{-1}$) and a higher area in contact with the flowing liquid, as proposed by Almenglo et al. [15].

Table 2. Removal efficiencies at different trickling liquid velocity (*TLV*s) and empty bed residence time (*EBRT*).

TLV **($m \cdot h^{-1}$)**	***EBRT*** **(s)** [1]		
	600	**200**	**120**
5.09	99.39	84.73	79.31
10.18	99.24	93.08	83.06
15.27	99.53	97.65	92.13

[1] The H_2S *IL*s were 35.1±1.5, 109.1±11.7 and 172.4±3.4 $gS \cdot m^{-3} \cdot h^{-1}$, for 600, 200 and 120 s, respectively.

Consequently, the influence of the nitrate concentration in the recirculating liquid on the H_2S *RE* was dependent of two factors: the H_2S *IL* and the *TLV*. A higher *TLV* level supplies a higher nitrate availability in the biofilm. *TLV* has usually been kept constant in anoxic BTFs between 10 [22] and 15 [23] $m \cdot h^{-1}$, but for a high H_2S *IL* it would be interesting to study the effect of this parameter. As in aerobic BTFs, where *TLV* is a key operational variable, in aerobic BTFs the regulation of *TLV* improves the oxygen mass transfer along the packed bed [24]. Fernández et al. [6] studied the effect of the *TLV* (2–20.5 $m \cdot h^{-1}$) on H_2S *RE* in an anoxic BTF, for H_2S *ILs* from 93 to 201 $gS \cdot m^{-3} \cdot h^{-1}$, packed with open pore polyurethane foam (the same support material as used in this study). It was found that there was no discernable influence for *TLV* values higher than 5 $m \cdot h^{-1}$ for H_2S *IL* values below 157 $gS \cdot m^{-3} \cdot h^{-1}$. However, at an H_2S *IL* of 201 $gS \cdot m^{-3} \cdot h^{-1}$ it was observed that *TLV* values below 15 $m \cdot h^{-1}$ produced a significant decrease in the H_2S *RE* from 92 to 85% at 4.5 $m \cdot h^{-1}$. On using polypropylene Pall rings [25] the optimal *TLV* was also 15 $m \cdot h^{-1}$ at high H_2S *IL* (>201 $gS \cdot m^{-3} \cdot h^{-1}$) although *TLV* did not have any effect at low H_2S *IL* (< 78.4 $gS \cdot m^{-3} \cdot h^{-1}$). Zeng et al. [3] studied the effect of *TLV* between 2.63 an 9.47 $m \cdot h^{-1}$ (H_2S *IL* < 86.92 $gS \cdot m^{-3} \cdot h^{-1}$) and achieved an efficient removal of H_2S for the lowest *TLV*, probably due to the larger height-diameter (*H/D*) ratio (10.9) and the higher *EBRT* (342 s). A high *H/D* ratio and a low *EBRT* improve the gas-liquid mass transfer [26] but increase the installation cost due to the higher pressure drop [27] and the higher volume of the packed bed.

The statistical results for the '*C model*' show the significance and high predictability of the regression model. The R-squared was 95.77%, the residual standard deviation was 0.1784 and the mean absolute error was 0.1224. The Durbin–Watson statistic was 1.00088 (p-value = 0.0001) and this shows a possible autocorrelation in the sample with a significance level of 5.0%. Moreover, the plot of residual versus predicted values (Figure 4a) does not show any patterns and we can assume a good correlation between

the model prediction and the experimental results. The second-order polynomial model fitted with calibration data is represented by Equation (11).

$$\begin{aligned} C_{G,H2S} = {} & -0.27436 + 0.0203426{\cdot}TLV + 0.0203127{\cdot}IL - 0.00935431{\cdot}\left[N\text{–}NO_3^-\right] \\ & -0.00120525{\cdot}TLV^2 - 0.000824025{\cdot}TLV{\cdot}IL + 0.000411032 \\ & {\cdot}TLV{\cdot}\left[N\text{–}NO_3^-\right] + 0.00000476214{\cdot}IL^2 - 0.0000513469{\cdot}IL \\ & {\cdot}\left[N\text{–}NO_3^-\right] + 0.0000617476{\cdot}\left[N\text{–}NO_3^-\right]^2 \end{aligned} \quad (11)$$

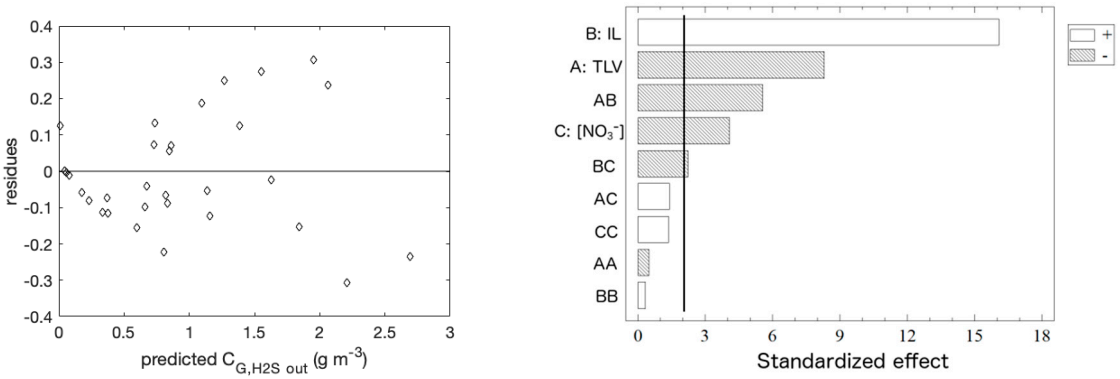

(**a**) (**b**)

Figure 4. Analysis for the '*C model*': Residual versus predicted (**a**) and Pareto chart (**b**).

As can be seen in Figure 4b, the most influential factor on the outlet H_2S concentration was the H_2S *IL* (p-value $2.26{\cdot}10^{-8}$). Moreover, the *TLV* and nitrate concentration had a negative effect on the outlet H_2S concentration with p-values of $5.26{\cdot}10^{-14}$ and $5.34{\cdot}10^{-4}$, respectively. It is interesting to note that the interaction AB (*IL* and *TLV*) was significant (p-value $1.18{\cdot}10^{-5}$) and therefore the effect of one variable depended on the value of another. This behavior can be seen in Figure 3, where the *TLV* had an effect on the *RE* at high H_2S *IL* but not at low ones.

The response surface for the '*C model*' is shown in Figure 5. The model can be used to predict the factor limits to achieve a desired H_2S outlet concentration. Depending on the combustion engine company, the inlet H_2S limit is in the range 100–500 mg·Nm^{-3} (72–359 ppm_V at 25 °C) [28]. Therefore, for a nitrate concentration of 35.5 mgN-NO_3^-·L^{-1} and *TLV* of 15.27 m h^{-1} the maximum H_2S *IL* would be 66.72 and 119.75 gS·m^{-3}·h^{-1} for outlet H_2S concentrations of 72 and 359 ppm_V, respectively.

The statistical results for the '*EC model*' show a higher significance and predictability of the regression model when compared with the '*C model*'. The R-squared was 99.63%, the residual standard deviation was 2.545 and the mean absolute error was 1.646. The Durbin–Watson statistic was 1.7041 (p-value = 0.0626), although the p-value was higher than 5% there were no traces of autocorrelation—as verified by checking the residual plot (Figure 6a). The second-order polynomial model fitted with calibration data is represented by Equation (12).

$$\begin{aligned} EC = {} & 11.0413 - 2.30638{\cdot}TLV + 0.844035{\cdot}IL + 0.172511{\cdot}\left[N\text{–}NO_3^-\right] \\ & +0.090618{\cdot}TLV^2 + 0.0225828{\cdot}TLV{\cdot}IL - 0.00947479{\cdot}TLV \\ & {\cdot}\left[N\text{–}NO_3^-\right] - 0.00231493{\cdot}IL^2 + 0.00184907{\cdot}L{\cdot}\left[N\text{–}NO_3^-\right] \\ & -0.00194474{\cdot}\left[N\text{–}NO_3^-\right]^2 \end{aligned} \quad (12)$$

As can be seen in Figure 6b, the most influential factor on the *EC* was the H_2S *IL* (p-value $1.81{\cdot}10^{-28}$). Moreover, the *TLV* and nitrate concentration had a positive effect on the *EC* with p-values of $2.37{\cdot}10^{-11}$ and $1.38{\cdot}10^{-5}$, respectively. In this case, the interactions AB (*IL* and *TLV*) and BC (*IL* and nitrate

concentration) and the quadratic term (BB or IL^2) were more significant than the nitrate concentration. Therefore, H_2S *IL* and *TLV* had a greater effect on the *EC* than the nitrate concentration.

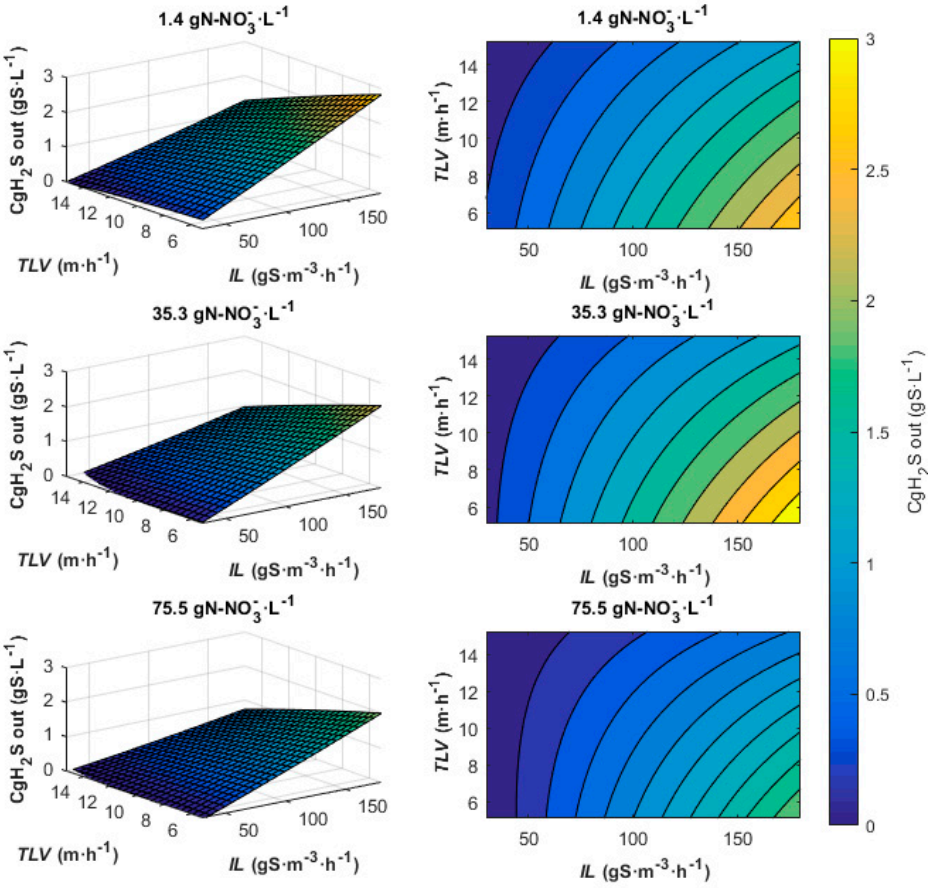

Figure 5. Response surfaces for the '*C model*'.

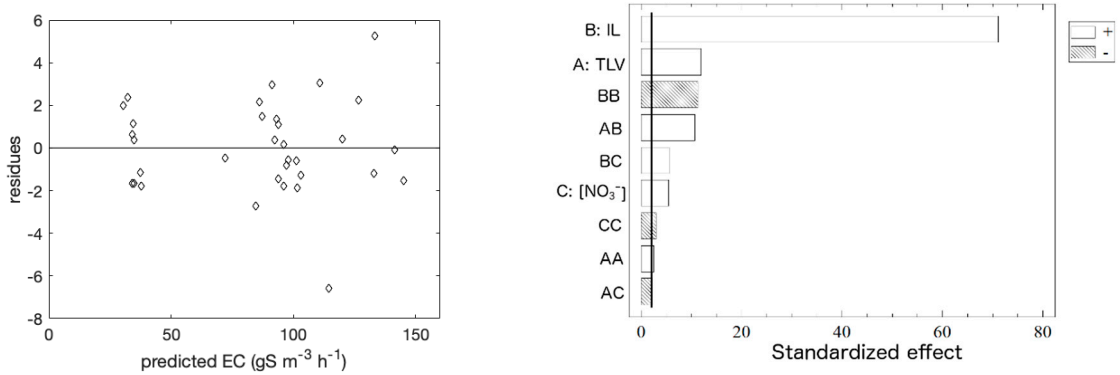

Figure 6. Analysis for the 'elimination capacity (EC) model': Residual versus predicted (**a**) and Pareto Chart (**b**).

The response surface for the '*EC model*' is shown in Figure 7. As expected, for high H_2S *IL* (>109.1 ± 11.7 $gS{\cdot}m^{-3}{\cdot}h^{-1}$) or high biogas flow rate (F_G > 3 $m^3{\cdot}h^{-1}$) an increase in *EC* was observed when the nitrate concentration and *TLV* were increased.

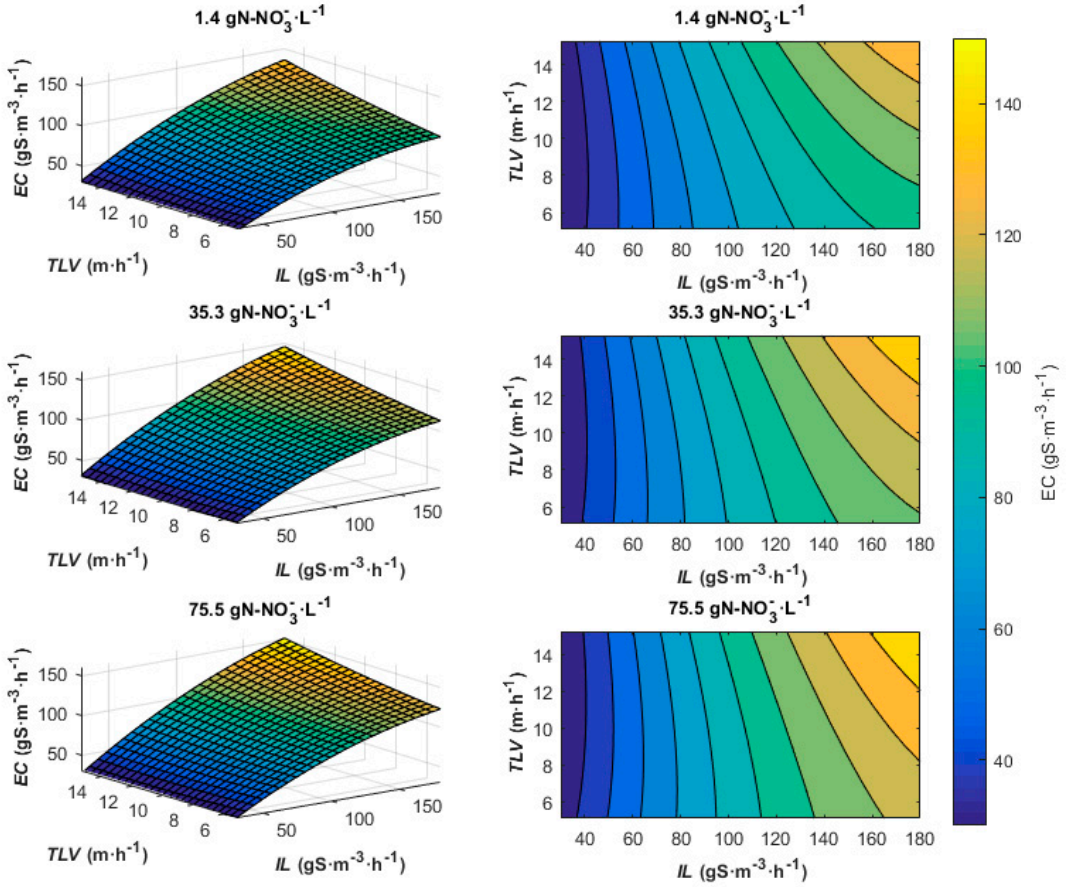

Figure 7. Response surface for the '*EC model*'.

A sensitivity analysis was performed by calculating the partial derivative in both models [29]. The maximum and minimum values for the variation of estimated variables corresponding to each factor are provided in Table 3. For the '*C model*' the maximum negative effect corresponded to a *TLV* of –0.1579 $(gS{\cdot}m^{-3})/(m{\cdot}h^{-1})$ and the maximum positive effect was for an H_2S *IL* of 0.0177 $(gS{\cdot}m^{-3})/(gS{\cdot}m^{-3}{\cdot}h^{-1})$. However for the '*EC model*' the maximum effects were due to *TLV* values of –1.252 $(gS{\cdot}m^{-3})/(m{\cdot}h^{-1})$ and 4.3303 $(gS{\cdot}m^{-3})/(m{\cdot}h^{-1})$.

Table 3. Sensitivity analysis.

Factor	*'C Model'*		*'EC Model'*	
	Maximum	**Minimum**	**Maximum**	**Minimum**
TLV	0.0078	–0.1579	4.3303	–1.252
IL	0.0177	0.0045	1.1553	0.1657
[N-NO_3^-]	0.0038	–0.159	0.4363	–0.1801

3.2. Ottengraf's Model

The concentration profiles along the bed height were analyzed using Ottengraf's model, without nitrate concentration limitations, for H_2S *IL* values between 33 and 176 $gS{\cdot}m^{-3}{\cdot}h^{-1}$ and *TLV* values between 5.09 and 15.27 $m{\cdot}h^{-1}$. The linear adjustments are provided in Table 4 according to the following simplifications: controlled by zero-order diffusion, zero-order kinetic and first-order kinetic. The behavior of the concentration profile for 5.09 $m{\cdot}h^{-1}$ and 130 and 170 $gS{\cdot}m^{-3}{\cdot}h^{-1}$ could be explained using a zero-order simplification for diffusion or kinetic. However, for all other conditions the

first-order kinetic simplification can be applied. The kinetic constant was in the range between 0.0025 and 0.0092 s^{-1}.

Table 4. Adjustments using Ottengraf's model.

IL ($gS \cdot m^{-3} \cdot h^{-1}$)	*TLV* ($m \cdot h^{-1}$)	Zero-Order Diffusion		Zero-Order Kinetic		First-Order Kinetic	
		r^2	k (s^{-1})	r^2	k (s^{-1})	r^2	k (s^{-1})
36	5.09	0.62	0.0018	0.3	0.012	0.95	0.008
35	10.18	0.57	0.0018	0.26	0.012	0.92	0.0087
33	15.27	0.52	0.0018	0.22	0.011	0.93	0.0092
130	5.09	0.95	0.0011	0.94	0.011	0.93	0.0031
108	10.18	0.91	0.0012	0.82	0.01	0.93	0.0036
104	15.27	0.93	0.0014	0.77	0.01	0.96	0.0057
170	5.09	0.97	0.0009	0.96	0.0079	0.96	0.0025
176	10.18	0.88	0.001	0.79	0.0091	0.93	0.0029
167	15.27	0.86	0.0011	0.74	0.0092	0.95	0.0034

To our knowledge, Ottengraf's model has not be applied to biogas desulfurization, although studies on H_2S removal from air have been modeled using Ottengraf's model [30–33].

Jin et al. [32] found that the zero-order kinetic limitation described the outlet H_2S concentration (*TLV* of 0.62 $m \cdot h^{-1}$ and a maximum H_2S *IL* around 30 $gS \cdot m^{-3} \cdot h^{-1}$). Oyarzún et al. [30] applied zero-order diffusion equations for an inlet H_2S concentration below Ks (Monod saturation constant) and zero-order kinetic equation and inlet concentration above Ks. The microbial kinetic of the biotrickling filter presented in this work can be described by a Haldane model [15], with an affinity constant for sulfide (Ks) of 8.4 $gS \cdot m^{-3}$ and a gas concentration in equilibrium of 1.28 $gS \cdot m^{-3}$. This concentration is considerably lower than the minimum inlet concentration employed in this work (5.55 $gS \cdot m^{-3}$). Therefore, the study was carried out at an inlet H_2S concentration higher than Ks with a first-order kinetic as obtained by Oyarzún et al. [30].

4. Conclusions

The influence of the nitrate concentration was dependent on *TLV* and H_2S *IL*, with its influence increasing for lower *TLV* and higher H_2S *IL*. The empirical models obtained by the response surface methodology for the factorial design of three factors at three levels (3^3) were able to predict the outlet H_2S concentration and the *EC* with a R-squared of 95.77% and 99.63% without autocorrelation. The most influential factors on the outlet H_2S concentration and *EC* were the H_2S *IL* and *TLV*, with the nitrate concentration being less significant. For biogas use in a CHP system the maximum H_2S *IL* should be between 66.72 and 119.75 $gS \cdot m^{-3} \cdot h^{-1}$ (*TLV* of 15.27 $m \cdot h^{-1}$ and nitrate concentration of 35.5 $mgN\text{-}NO_3^- \cdot L^{-1}$). Moreover, Ottengraf's model was applied successfully considering a first-order kinetic limitation simplification with an R-squared above 0.92.

Author Contributions: Research design, D.C. and M.R.; methodology, F.A. and M.R.; investigation, F.A.; writing—original draft preparation, F.A.; writing—review and editing, M.R.; supervision, D.C. and M.R.; funding acquisition, D.C. and M.R.

Funding: This research was funded by MINISTERIO DE ECONOMÍA Y COMPETITIVIDAD, grant number CTM2009-14338-C03-02 and the Research Result Transfer Office of the University of Cádiz, grant number PROTO-05-2010.

Acknowledgments: The authors wish to express sincere gratitude to the WWTP "UTE EDAR Bahía de Cádiz" for allowing us to install the biotrickling filter in their plant.

Conflicts of Interest: The authors declare no conflict of interest.

References

1. European Commission. *A Clean Planet for All a European Strategic Long-Term Vision for a Prosperous, Modern, Competitive and Climate Neutral Economy*; COM (2018) 773 Final; European Commission: Brussels, Belgium, 2018; pp. 1–25.
2. Cano, P.I.; Colón, J.; Ramírez, M.; Lafuente, J.; Gabriel, D.; Cantero, D. Life cycle assessment of different physical-chemical and biological technologies for biogas desulfurization in sewage treatment plants. *J. Clean. Prod.* **2018**, *181*, 663–674. [CrossRef]
3. Zeng, Y.; Luo, Y.; Huan, C.; Shuai, Y.; Liu, Y.; Xu, L.; Ji, G.; Yan, Z. Anoxic biodesulfurization using biogas digestion slurry in biotrickling filters. *J. Clean. Prod.* **2019**, *224*, 88–99. [CrossRef]
4. Valle, A.; Fernández, M.; Ramírez, M.; Rovira, R.; Gabriel, D.; Cantero, D. A comparative study of eubacterial communities by PCR-DGGE fingerprints in anoxic and aerobic biotrickling filters used for biogas desulfurization. *Bioprocess Biosyst. Eng.* **2018**, *41*, 1165–1175. [CrossRef] [PubMed]
5. Montebello, A.M.; Fernández, M.; Almenglo, F.; Ramírez, M.; Cantero, D.; Baeza, M.; Gabriel, D. Simultaneous methylmercaptan and hydrogen sulfide removal in the desulfurization of biogas in aerobic and anoxic biotrickling filters. *Chem. Eng. J.* **2012**, *200–202*, 237–246. [CrossRef]
6. Fernández, M.; Ramírez, M.; Gómez, J.; Cantero, D. Biogas biodesulfurization in an anoxic biotrickling filter packed with open-pore polyurethane foam. *J. Hazard. Mater.* **2014**, *264*, 529–535. [CrossRef] [PubMed]
7. Fortuny, M.; Baeza, J.; Gamisans, X.; Casas, C.; Lafuente, J.; Deshusses, M.; Gabriel, D. Biological sweetening of energy gases mimics in biotrickling filters. *Chemosphere* **2008**, *71*, 10–17. [CrossRef]
8. Wainwright, J.; Mulligan, M. *Environmental Modelling: Finding Simplicity in Complexity*, 2nd ed.; John Wiley & Sons, Inc.: Hoboken, NJ, USA, 2013; ISBN 978-0-470-74911-1.
9. Ottengraf, S.; Rehm, H.; Reed, G. Exhaust gas purification. In *Biotechnology—A Comprehensive Treatise*; Verlag Chemie: Weinheum, Germany, 1986; Volume 8, pp. 426–452.
10. Shareefdeen, Z.; Baltzis, B.; Oh, Y.; Bartha, R. Biofiltration of Methanol Vapor. *Biotechnol. Bioeng.* **1993**, *41*, 512–524. [CrossRef]
11. Baltzis, B.; Wojdyla, S.; Zarook, S. Modeling biofiltration of VOC mixtures under steady-state conditions. *J. Environ. Eng.* **1997**, *123*, 599–605. [CrossRef]
12. Soreanu, G. Insights into siloxane removal from biogas in biotrickling filters via process mapping-based analysis. *Chemosphere* **2016**, *146*, 539–546. [CrossRef]
13. Soreanu, G.; Falletta, P.; Béland, M.; Edmonson, K.; Ventresca, B.; Seto, P. Empirical modelling and dual-performance optimisation of a hydrogen sulphide removal process for biogas treatment. *Bioresour. Technol.* **2010**, *101*, 9387–9390. [CrossRef]
14. López, L.; Dorado, A.; Mora, M.; Gamisans, X.; Lafuente, J.; Gabriel, D. Modeling an aerobic biotrickling filter for biogas desulfurization through a multi-step oxidation mechanism. *Chem. Eng. J.* **2016**, *294*, 447–457. [CrossRef]
15. Almenglo, F.; Ramírez, M.; Gómez, J.; Cantero, D.; Gamisans, X.; Dorado, A. Modeling and control strategies for anoxic biotrickling filtration in biogas purification. *J. Chem. Technol. Biotechnol.* **2016**, *91*, 1782–1793. [CrossRef]
16. Almenglo, F.; Ramírez, M.; Gómez, J.; Cantero, D. Operational conditions for start-up and nitrate-feeding in an anoxic biotrickling filtration process at pilot scale. *Chem. Eng. J.* **2016**, *285*, 83–91. [CrossRef]
17. Clesceri, L.S.; Greenberg, A.; Eaton, A. *Standard Methods for the Examination of Water and Waste Water*, 20th ed.; American Public Health Association, American Water Works Association, Water Environment Federation: Washington, DC, USA, 1999; ISBN 0875532357.
18. Veljković, V.B.; Veličković, A.V.; Avramović, J.M.; Stamenković, O.S. Modeling of biodiesel production: Performance comparison of box–Behnken, face central composite or full factorial design. *Chin. J. Chem. Eng.* **2018**. [CrossRef]
19. Montgomery, D.C. *Design and Analysis of Experiments*, 5th ed.; John Wiley & Sons, Inc.: Hoboken, NJ, USA, 2001; p. 208. ISBN 0-471-31649-0.
20. Ottengraf, S.; Oever, V.A. Kinetics of organic compound removal from waste gases with a biological filter. *Biotechnol. Bioeng.* **1983**, *25*, 3089–3102. [CrossRef] [PubMed]
21. Onda, K.; Takeuchi, H.; Okumoto, Y. Mass transfer coefficients between gas and liquid phases in packed columns. *J. Chem. Eng. Jpn.* **1968**, *1*, 56–62. [CrossRef]

22. López, L.R.; Brito, J.; Mora, M.; Almenglo, F.; Baeza, J.A.; Ramírez, M.; Lafuente, J.; Cantero, D.; Gabriel, D. Feedforward control application in aerobic and anoxic biotrickling filters for H_2S removal from biogas. *J. Chem. Technol. Biotechnol.* **2018**, *93*, 2307–2315. [CrossRef]
23. Brito, J.; Valle, A.; Almenglo, F.; Ramírez, M.; Cantero, D. Progressive change from nitrate to nitrite as the electron acceptor for the oxidation of H_2S under feedback control in an anoxic biotrickling filter. *Biochem. Eng. J.* **2018**, *139*, 154–161. [CrossRef]
24. López, L.R.; Bezerra, T.; Mora, M.; Lafuente, J.; Gabriel, D. Influence of trickling liquid velocity and flow pattern in the improvement of oxygen transport in aerobic biotrickling filters for biogas desulfurization. *J. Chem. Technol. Biotechnol.* **2016**, *91*, 1031–1039. [CrossRef]
25. Fernández, M.; Ramírez, M.; Pérez, R.; Gómez, J.; Cantero, D. Hydrogen sulphide removal from biogas by an anoxic biotrickling filter packed with Pall rings. *Chem. Eng. J.* **2013**, *225*, 456–463. [CrossRef]
26. Ordaz, A.; Figueroa-González, I.; San-Valero, P.; Gabaldón, C.; Quijano, G. Effect of the height-to-diameter ratio on the mass transfer and mixing performance of a biotrickling filter. *J. Chem. Technol. Biotechnol.* **2018**, *93*, 121–126. [CrossRef]
27. Lebrero, R.; Gondim, A.; Pérez, R.; García-Encina, P.A.; Muñoz, R. Comparative assessment of a biofilter, a biotrickling filter and a hollow fiber membrane bioreactor for odor treatment in wastewater treatment plants. *Water Res.* **2014**, *49*, 339–350. [CrossRef] [PubMed]
28. Ramírez, M.; Gómez, J.; Cantero, D.; Ramírez, M.; Gómez, J.; Cantero, D. Biogas: Sources, Purification and Uses. In *Hydrogen and Other Technologies*; Studium Press LLC: Houston, TX, USA, 2015; Volume 11, pp. 296–323. ISBN 978-1-626990-72-2.
29. Koda, M.; Dogru, A.H.; Seinfeld, J.H. Sensitivity analysis of partial differential equations with application to reaction and diffusion processes. *J. Comput. Phys.* **1979**, *30*, 259–282. [CrossRef]
30. Oyarzún, P.; Arancibia, F.; Canales, C.; Aroca, G.E. Biofiltration of high concentration of hydrogen sulphide using *Thiobacillus thioparus*. *Process Biochem.* **2003**, *39*, 165–170. [CrossRef]
31. Jaber, M.; Couvert, A.; Amrane, A.; Rouxel, F.; Cloirec, P.; Dumont, E. Biofiltration of H_2S in air—Experimental comparisons of original packing materials and modeling. *Biochem. Eng. J.* **2016**, *112*, 153–160. [CrossRef]
32. Jin, Y.; Veiga, M.C.; Kennes, C. Effects of pH, CO_2, and flow pattern on the autotrophic degradation of hydrogen sulfide in a biotrickling filter. *Biotechnol. Bioeng.* **2005**, *92*, 462–471. [CrossRef] [PubMed]
33. Shareefdeen, Z.M.; Ahmed, W.; Aidan, A. Kinetics and Modeling of H_2S Removal in a Novel Biofilter. *Adv. Chem. Eng. Sci.* **2011**, *1*, 72–76. [CrossRef]